Available online at www.sciencedirect.com
ScienceDirect
Journal of Nuclear Materials 363–365 (2007) 32–40
journal of nuclear materials
www.elsevier.com/locate/jnucmat

The implications of mixed-material plasma-facing surfaces in ITER

R.P. Doerner *

Center for Energy Research, University of California at San Diego, 9500 Gilman Drive, La Jolla, CA 92093-0417, USA

Abstract

In all plasma-confinement devices, material eroded from plasma-facing surfaces will be transported and redeposited at other, sometimes remote, locations. If the plasma-facing material in a device consists of more than a single element there is a high probability that the composition of the plasma-facing surfaces will evolve over time and may exhibit plasma-interaction properties much different from the originally installed material. These plasma-created materials, or mixed materials, are the subjects of this review paper which focuses on the ITER relevant mix of materials, namely carbon, tungsten and beryllium. Knowledge concerning the formation conditions, erosion behavior and hydrogen isotope retention properties of each binary combination of materials is described. Where available information concerning tertiary combinations of materials is discussed.

PACS: 52.40.Hf

Keywords: ITER; Erosion and deposition; Chemical erosion; Codeposition; Deuterium inventory

1. Introduction

The plasma-facing surfaces provide the boundary conditions that govern the performance of any magnetically confined plasma device. The importance of these material surfaces will continue to increase as devices push toward higher and higher power and longer discharge duration. In machines that operate using a mixture of deuterium and tritium fuel, many safety aspects of operational capability will be determined by the behavior of the plasma-facing components and materials. For these reasons, the designers of the ITER project [1] have settled on a multi-material solution for their plasma-facing surfaces.

Unfortunately, the properties of the materials used in design calculations are usually the values associated with the 'as-received' material. In the proximity of high temperature plasma, material erodes from plasma-facing materials in one location and is transported to other locations throughout the device. The transported material may then be deposited on, or implanted into, other materials. In 1978, S.A. Cohen succinctly described this process [2] as 'The wall may be eroded due to a variety of possible mechanisms which generate

* Tel.: +1 619 534 7830; fax: +1 619 534 7716.
E-mail address: rdoerner@ucsd.edu

0022-3115/$ - see front matter
doi:10.1016/j.jnucmat.2006.12.059

plasma- impurities, and subsequent plasma transport of impurities may deposit material onto the wall. This modified surface of the wall is the wall component subjected to subsequent plasma–wall interactions; it is both a source and sink of plasma-impurities and the working gas.' The term 'mixed material' has recently been coined to describe the resultant, plasma-created surface. Even though the importance of this issue was recognized almost three decades ago, detailed investigations of plasma-interactions with surfaces composed of more than a single element began only during the last decade or so.

Although plasma-altered surfaces have been observed in many confinement devices, once their compositions have been characterized, they have been largely ignored. The exceptions to this general statement seem to be those machines that have operated with a mixture of deuterium and tritium (D/T) fuel. The primary reason for the increased attention in D/T machines was the need to understand the tritium retention locations and characteristics throughout the devices. In the late 1980s, the term 'tokamakium' was used to refer to plasma-created mixed-material surfaces found in TFTR [3]. Although TFTR was primarily an all-carbon machine, the impurity content and morphology of the mixed-material surfaces was found to reflect changes in the operational history of the device.

The other major D/T facility, JET, has also spent considerable effort on understanding the behavior of mixed-material surfaces [4–6]. In the JET device both carbon and beryllium were used together as plasma-facing materials and the resultant surfaces show considerable mixing between the two elements. Again, compositional changes in the depth profiles of the mixed-material surfaces can be correlated to the operational history of the machine [7]. The interrelated nature of the machine performance and the resultant plasma-facing surfaces indicates the importance of predicting the behavior of mixed-material surfaces in ITER prior to operating the device, both for facility safety requirements, as well as from the point of view of plasma performance and the achievement of the goals of the overall ITER project.

The conclusions derived from many active areas of research are needed to be able to accurately predict which mixed-materials surfaces will form in which regions of the ITER plasma-facing surfaces. The creation of mixed-material surfaces will depend on many factors that determine the arrival and loss rate of material from those surfaces [8]. In order to know the arrival rate of an impurity species in the plasma at a given surface, one must understand the transport properties of the scrape-off layer (SOL) plasma. Edge plasma-turbulence induces cross-field transport, resulting in both diffusive-like and convective plasma-transport into and through the SOL region [9]. The magnitude of convectively transported flux to the first wall, commonly called blob transport [10], is actively being investigated. In addition, large SOL plasma-flows have been measured but not yet explained in several plasma-confinement machines [8]. Finally, erosion terms due to asymmetries and off-normal events, such as ELMs [11], also contribute to the distribution of impurities throughout the ITER vessel. From the surface loss rate perspective, the surface temperature of the bombarded material is a critical factor in determining the chemical processes acting in the surface [12] and the resultant morphology of the exposed surface [13]. The creation of mixed-material compounds in the surface of plasma-exposed materials can potentially alter the thermal conductivity of these surfaces and thereby make reliable predictions of the surface temperature doubtful.

In spite of the large uncertainties associated with the locations where mixed materials will form in ITER, it can be predicted with some certainty that mixed-material surfaces will occur. Data on the characteristics and behavior of mixed-material surfaces is urgently needed by the ITER design team to try to anticipate and possibly mitigate any undesirable effects. Since ITER is presently designed with a beryllium first wall, tungsten armor in the baffle and divertor regions, and carbon strike point plates, this paper focuses on the mixed-material characteristics of these three materials. The present understanding of each of the binary systems, C/W, Be/C and Be/W, is described, including a discussion of the added complexity of tertiary systems incorporating oxygen into the mix. For each system, the formation conditions, the erosion characteristics and the hydrogen isotope retention properties of the mixed materials are described.

2. Carbon/tungsten system

The carbon–tungsten mixed-material system is probably the most widely studied system, both experimentally and computationally. In 1991, experiments detected an interesting and unexpected reversal in the mass loss from room temperature

tungsten samples bombarded with carbon ion beams at normal incidence [14]. Kinetics based Monte-Carlo codes using a binary collision approximation (BCA), such as TRIDYN [15] and EDDY [16], have had success predicting the sputtering behavior of tungsten surfaces exposed to such a flux of energetic carbon ions. A comparison of the modeling results and the experimental data are shown in Fig. 1. The models track the changes in the composition of the implantation zone due to the bombardment of carbon ions. During the stopping process of the carbon ions, tungsten atoms can be sputtered from the initially pristine tungsten surface. The surface recession due to sputtering effectively acts to move the implanted carbon toward the surface. After some fluence, the initially implanted carbon ions will become part of the composition of the surface layer.

Once initially implanted carbon ions reach the new surface in the model, several effects occur which change the interaction of the incoming carbon with the now mixed-material surface. First, the reflection probability of the incoming ions decreases due to a decrease in the mass difference between the projectile and the 'average' target species. The mass loss of tungsten from the surface then decreases as the concentration of surface carbon increases which is of course coupled to an increase in the loss rate of carbon from the surface. However, since the self-sputtering yield of carbon at normal incidence is always below unity [17], the overall mass of the sample begins to increase. At sufficiently large fluence, the sample will begin to experience a net mass gain.

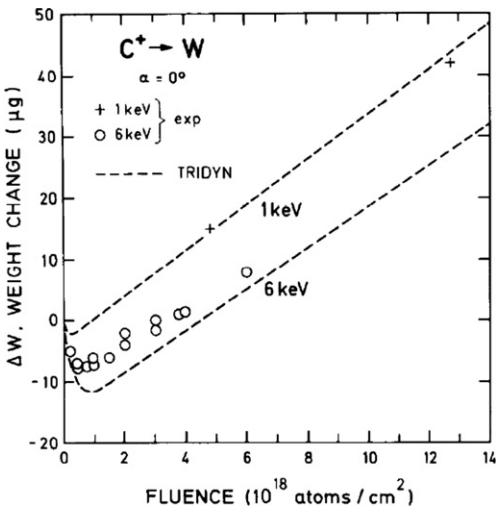

Fig. 1. Comparison of modeling and experimental data showing fluence dependent weight loss from a tungsten sample exposed to carbon ion bombardment (reproduced with permission from [14]).

The effect of the incident angle of the carbon ions can be used to verify the understanding obtained from the model. By simply increasing the angle between the incident ions and the surface normal, one can obtain a condition where the self-sputtering yield of carbon is larger than unity. Under such condition, both the experiment and the model show a continuous decrease in the mass of bombarded tungsten samples [14].

To properly predict the behavior of material systems in confinement devices, it is necessary to include effects that become important at elevated surface temperature. While temperature dependent effects are not included in these models, it is possible to couple the kinetics models with subroutines that allow variations of the composition in surface layers to include effects, such as diffusion. This has been done [18–20] and the comparison of the model to experiments can be quite good. However, in each case the diffusion coefficients needed to reproduce the experimental data are smaller than the values prescribed in the literature (see list of references in [14]).

One possible explanation for this behavior begins to shed light on the complexity of modeling plasma-created mixed-material surfaces. In addition to activating diffusion at elevated sample temperature, reactions between the substrate material and the implanted carbon species occur, resulting in the formation of carbides. Depending on the substrate material involved, carbides with different bonding characteristics are observed [21]. Carbides that form ionic bonds, such as Be_2C, are very stable against diffusion of carbon. Similarly, but to a somewhat lesser extent, covalent carbides, such as SiC, also resist diffusion of the carbon component. However, carbides that form with carbon filling the regions in the close packed metal lattice, such as WC, tend to be more favorable for diffusion since for diffusion to occur no direct bonds between the metal and the carbon must be broken in the process [21]. Effects such as this demonstrate the importance of including chemical effects in the models to accurately predict the behavior of plasma-exposed surfaces. It may not be adequate to search the literature for data obtained during measurements performed under equilibrium, or trace concentration, conditions and then attempt to use that data to model the behavior of materials exposed to plasma where the situation may be far from equilibrium and the

concentrations of species may not be negligibly small [20].

Chemical bonding in the surface plays a large role in determining the behavior of the plasma–surface interactions. For the case of carbide formation in tungsten, during the annealing of carbon films on tungsten, the carbon begins to strongly react and form carbides with the tungsten substrate at around 900 K [22] (although some small amount of carbide exists at the carbon–tungsten interface even at room temperature). Carbide interlayers have also been observed between carbon layers deposited on tungsten substrates when exposed to plasma-containing carbon impurities [23]. The chemical erosion properties of a plasma-facing surface that has reacted to form even a partial carbide layer, or when experimentally examining the plasma-interaction behavior of a fully carbidic surface, is completely different from chemical erosion properties of graphite. For a fully carbidized sample the CH_4 production rate drops by at least an order of magnitude compared to that of graphite [24,25]. Presumably the presence of the carbidic bonding inhibits the production rate of C–H bond formation.

From the modeling perspective, properly including chemical effects becomes even more apparent when the BCA approach to the W/C system is expanded to include the effects associated with a large flux of hydrogen to the system. It is again possible to obtain good agreement between simulation and experimental data [26], but the agreement is obtained after the fact and could not be considered predictive. Determining the appropriate value to use for the chemical erosion yield of carbon in the ITER situation is particularly difficult given the wide range of measured values in the literature and its dependence on parameters such as temperature [27], flux [28], surface composition [25,26] and possibly other variables.

A final complication worth mentioning is the possibility, or perhaps even likelihood, of additional elements being present in a confinement device scenario. Exploration of the tertiary W/C/O system has shown that the presence of oxygen in a mixed tungsten–carbon surface can inhibit, or in some cases even prevent the formation of tungsten carbide [22]. The presence of oxygen allows for the formation of volatile species, CO and CO_2, which deplete carbon from the surface and influence the amount of carbon available for reaction with surface tungsten. At this stage it is still speculation to attempt to estimate the amount of oxygen that may be present in the ITER vacuum system, although it should be noted that baking in an oxygen atmosphere is being considered as a possible technique to remove tritium-containing codeposits in ITER [29].

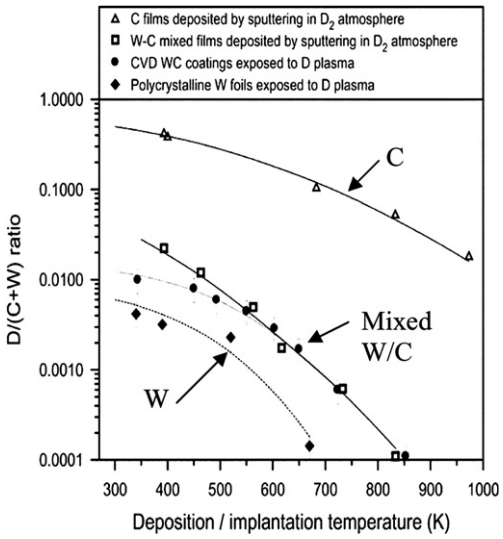

Fig. 2. Comparison of hydrogen isotope retention between pure carbon and tungsten surfaces to the retention in mixed W/C material (reprinted with permission from [32]).

An important variable to quantify from a safety perspective is the fuel retention capability of mixed-material plasma-facing surfaces. Again the difficulty becomes how to relate the behavior of plasma-created mixed materials to other measurements. In vacuum annealing measurements of tungsten coated with an amorphous C:H layer, the formation of W_2C is accompanied by a release of hydrogen from the surface [30]. The conclusion drawn is that when a mixed W–C surface forms on a plasma-facing surface it will retain little fuel atoms. However, during deuterium ion beam irradiation studies of a W_2C sample the measured deuterium retention level was between that measured from a clean tungsten surface and a fully carbon covered tungsten surface [31]. Similar measurements obtaining retention levels of mixed W–C surfaces lying between that of carbon surfaces and tungsten surfaces are shown in Fig. 2 and have been reported by several authors [24,32,33].

3. Beryllium/carbon system

Material eroded from the ITER first wall will be ionized in the scrape-off layer plasma and tend to

flow along the magnetic field toward the divertor. Recent modeling of the transport of eroded material in ITER shows that significant amounts of beryllium may be deposited on the baffle and divertor areas [34].

To first order, the processes used to describe the interaction of carbon ion beams with beryllium samples [35] are similar to the interaction of carbon with tungsten. Initially, the bombardment results in a beryllium carbide rich implantation zone that, due to surface erosion, migrates and eventually become the surface layer. The change in surface layer composition directly effects the composition of material leaving the surface, however, there is a subtle difference between tungsten and beryllium interactions with the incident carbon ions. For the W–C system, a primary mechanism responsible for building up carbon layers is the change in the reflection probability for the incident ions due to a lower average mass of the target surface. In the case of the Be–C system, the reflection coefficient does not change appreciably due to the development of the beryllium carbide layer. The effective binding energy calculated by the code changes more dramatically in the Be–C case then in the W–C case and this changes the calculated Be surface loss rate. The TRIDYN code varies the effective surface binding energy linearly between the mean value of the two elemental binding energies and the value of the pure element based on the composition of the layer [36]. In the case of beryllium, $E_b \sim 3.3$ eV, and carbon, $E_b \sim 7.4$ eV, this is a more dramatic effects than between tungsten, $E_b \sim 8.9$ eV and carbon [37]. Once the surface recession rate is reduced more carbon will build up in the implantation zone and eventually a carbon rich layer results. Calculations based on this mathematical expression for the surface binding energy do a good job of replicating ion beam sputtering results [38,39]. Similar behavior is predicted for Be ions impinging on a carbon target [40].

While the approximation used to simulate surface binding energies of mixed surfaces appears to work well at higher energy, where the sputtering yield does not vary dramatically with the value for the binding energy, it appears that a more rigorous treatment is needed in the near-threshold-energy range when large amount of deuterium are also present in the surface. The PISCES device has observed the formation of beryllium-rich layers on graphite targets exposed to deuterium plasma containing very small amounts (~0.1%) of beryllium impurities [41,42]. However, in the inverse Be–C system, namely carbon plasma contamination incident on Be samples, carbon-rich surfaces required a much larger (1–2%) incident impurity fraction to form [43]. While the equilibrium surface composition of the resultant plasma-exposed surfaces could be predicted [43,44] reasonably well using typical values for plasma–material interaction parameters in the literature, the temporal evolution of the surface composition could not be.

The surface of the plasma-exposed samples are observed to evolve over time frames that can be as long as thousands of seconds, or as short as seconds, depending on the plasma-experimental conditions [45]. The change in the composition of the surface is correlated to a reduction in the chemical erosion of the graphite sample. As in the case of tungsten carbide formation in a surface reducing the chemical erosion properties of the bound carbon, beryllium carbide formation in the surface of these samples appears to again be responsible for the reduction [46]. In the plasma-environment many parameters can have an influence on the formation of beryllium carbide layers, such as, incident Be flux, surface temperature, incident energy, etc. A systematic variation of plasma and target conditions has resulted in the development of a scaling law to describe the formation time of the beryllium-rich layers in the PISCES experiments [47].

The scaling law is a different approach, compared to using the kinetic Monte-Carlo models, to predicting the behavior of mixed-material surfaces. Application of this scaling to typical conditions expected in the ITER divertor provides an estimate of the fluence necessary to inhibit the production of hydrocarbons from the ITER divertor plates. If the extrapolation of this scaling law to ITER is valid, it predicts a beryllium-rich layer to form in approximately 5 ms [47] of ITER-type plasma-exposure. This formation time estimate is considerably shorter than the ELM frequency (~1 Hz) expected in ITER, which means that the Be–C mixed-material surfaces may be present most of the time on the ITER divertor plates.

Another issue being addressed in the beryllium-seeded plasma-experiments, is the robustness of the beryllium–carbide surfaces to the transient heating effects associated with ELM power losses in ITER. Previous measurements of the existence of thin aluminum layers (as a surrogate for beryllium layers) deposited on graphite and then subjected to extreme power loading revealed that the aluminum

did not ablate from the surface until the temperature of the surface exceeded the boiling point of aluminum [48]. While the PISCES-B heat pulsing experiments have not yet achieved a surface temperature exceeding the boiling temperature of beryllium ($T_{boil} = 2744$ K), or the decomposition temperature of beryllium carbide ($T_{Be_2C\ decomo.} \sim 2400$ K), they have shown that the protective Be layer forms faster while periodic heat pulses are applied to the samples during the course of the plasma-exposure [49]. The quicker suppression of chemical erosion from the plasma-exposed samples is in qualitative agreement with the predictions of the scaling law [47] previously described.

One complication to directly applying these results to predictions for the behavior of ITER is the composition of the incident ion flux to the surface. In measurements involving the tertiary mixed-material Be–C–O system, dramatically different results are obtained. Recall that the interaction of the two-component Be–C system resulted in the formation of a Be_2C layer, the bombardment of beryllium with CO^+ ion beams results in almost exclusive binding of the beryllium to the oxygen in the implantation zone [35,39]. The carbon atoms present are then bound up in C–C or C–O bonds. Once this implantation zone reaches the receding surface, the carbon is easily chemically eroded. The differences between these measurements and those described in the PISCES simulator relate to the amount of oxygen present in the incident ion flux. Depending on the level of oxygen present in ITER, the final behavior may lie somewhere between the two results described.

A trend similar to that observed with the W–C system with respect to hydrogen release is also exhibited during formation of beryllium carbide obtained by reacting a surface layer of amorphous C:D with a beryllium substrate, as shown in Fig. 3. Once the carbide reaction begins to occur, typically in the temperature range of 773–873 K, deuterium is released from the reacted material [50,51]. Again, such a result does not guarantee that Be_2C bombarded with energetic hydrogen isotopes will retain little of the incident particle fluence. Deuterium ion beam implantation into mixed Be–C layers showed higher retention in the mixed-material samples, compared to clean Be samples [52]. Retention measurements from plasma-created mixed-material targets also show larger retention in mixed Be–C layers compared to clean Be targets [43], but surprisingly mixed Be–C targets also show

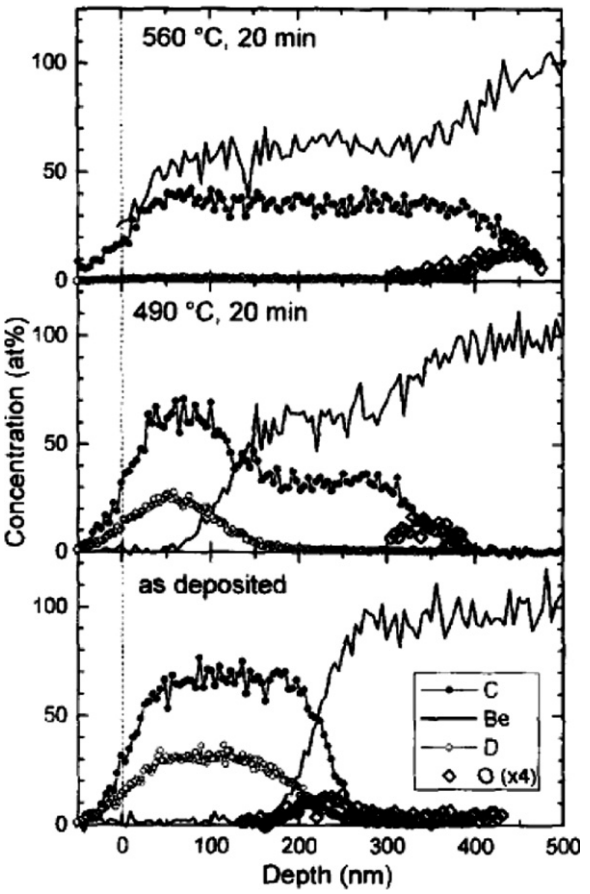

Fig. 3. Reaction with temperature of an amorphous C:D layer with a beryllium substrate (reprinted with permission from [51]). Deuterium in the codeposited C:D layer is released as beryllium carbide forms at higher temperature.

larger retention when compared with clean carbon targets exposed to identical plasma-discharges [46]. In both cases of plasma-created mixed Be–C (Be incident on C and C incident on Be) surfaces the differences in retention are largest during low surface temperature exposure. The differences in retention decrease as the exposure temperature increases.

For the ITER device, the dominant term driving the tritium inventory in the vessel is predicted to be codeposition of tritium with eroded material, rather than implantation and retention in plasma-exposed target surfaces [29]. The eroded material capable of codepositing will be determined by the mixed-material surfaces with which the plasma interacts. In measurements of codeposition of deuterium with a mixed Be–C–O layer [53], the deuterium concentration was observed to be similar to that of codeposition of deuterium with pure carbon. The hypothesis was that deuterium was coimplanting into a

growing BeO film, rather than codepositing with the smaller amount of carbon present in the films. Subsequent measurement seemed to confirm this hypothesis, as the measured deuterium content in coimplanted Be films seemed to scale with the cleanliness of the films produced [54]. During PISCES beryllium seeded plasma experiments when Be_2C surface layers form on mixed-material targets, the codepositing material is measured to consist almost exclusively of beryllium [55] with a varying amount of oxygen present in the coimplanted beryllium. However, during the PISCES codeposited material collection, films collected at higher temperature had decreasing amounts of deuterium retained in the films, yet also contained an increasing amount of oxygen. It has been suggested that the varying concentration of deuterium is governed by the energy of the incident deuterium during the coimplantation rather than by the oxygen content in the films [56].

While the mechanism governing the retention is still under investigation, certain information is already clear. First, if beryllium-rich layers form on ITER plasma-facing materials, then the codepositing material will consist primarily of beryllium. Second, although the level of codeposition, or coimplantation, in beryllium-rich layers at room temperature is similar to that expected in carbon-rich codeposits, the concentration decreases much more rapidly with temperature in beryllium codeposits than it does in carbon codeposits. And finally, it appears to be easier to remove the deuterium content in beryllium-rich codeposits at lower temperature than from carbon-rich codeposits. This last fact is shown in Fig. 4, where data from outgassing measurements of beryllium-rich codeposits [55] is replotted and compared to data from thermally desorbing carbon-rich codeposits [57]. Also indicated in the figure is the design value for the maximum bake temperature achievable in the ITER divertor (650 K) after the coolant is drained from the divertor components.

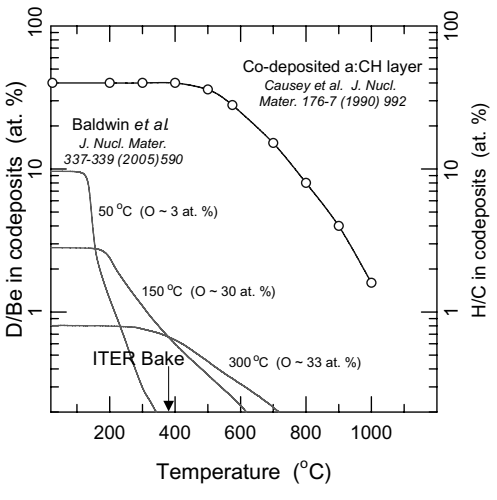

Fig. 4. Comparison of hydrogen isotope desorption characteristics from beryllium based and carbon based codeposits.

4. Beryllium/tungsten system

The third binary system of materials that is a concern for the ITER design is that of beryllium–tungsten alloys, so called tungsten beryllides. While the existence of these alloys (Be_2W, $Be_{12}W$ and $Be_{22}W$) has been known for some time [58], it is only recently that their importance has been recognized. The primary reason for concern stems from the beryllium plasma-seeding experiments carried out in the PISCES Laboratory. In the initial series of measurements the beryllium-supplying oven contained a tungsten crucible holding the molten beryllium. This crucible melted and destroyed the oven while operating at only about 1500 K [59]. The uncertainty associated with any possibility for a similar major malfunction in the ITER divertor region has brought significant new effort to this area. A detailed description of tungsten beryllides is presented in these proceedings [60] and so will not be repeated here.

The formation of beryllides will be governed by the conditions experienced by tungsten plasma-facing materials due to interaction with the incident plasma. Since the temperature of the surface must be fairly large (~1100 K or more) to allow significant growth of the alloy, the loss rate of beryllium from these surfaces will be impacted significantly by both thermal sublimation and thermally enhanced erosion of beryllium [61] from the material. A model has been proposed to describe plasma-conditions that should result in the formation of a beryllium layer on a plasma-exposed tungsten surface [62] and this model should provide insight into which surfaces in ITER might be most susceptible to beryllide formation.

While there is presently no data available concerning retention, or codeposition, of deuterium in Be/W alloys, one might expect that when and if these alloys form, the codeposited material will consist primarily of beryllium and the codeposition discussion presented in the previous section will hold. In addition

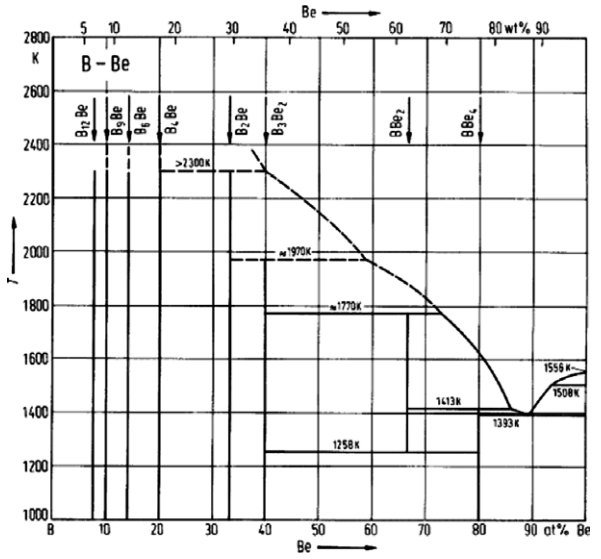

Fig. 5. Phase diagram of beryllium boride (reprinted with permission from [65]).

there has been little, if any, codeposition of deuterium with tungsten observed experimentally [63].

A final word of caution is perhaps in order with regard to similar consequences from unexpected mixed-material formation. There has been an ongoing discussion in the community about the necessity of designing a boronization system for possible use in ITER. Similar to the tungsten–beryllide alloys, tungsten–boride alloys exist [64] that have melting temperatures lower than that of elemental tungsten. In addition, beryllium–boride alloys could form on the beryllium first wall. The beryllium boride phase diagram, Fig. 5, shows that the mixed Be–B system can even have a melting temperature lower than that of elemental beryllium [65].

5. Summary

Due to the combination of materials employed in different locations in the ITER design there is a strong likelihood that some types of mixed materials will form on plasma-facing surfaces. This review has summarized present knowledge of each of the three binary mixed-material systems, C/W, Be/C and Be/W. The added complications associated with including the effects of oxygen, or hydrogen, in the mix have also been discussed. While no definitive conclusions can yet be drawn concerning the implication of mixed materials in ITER, there have been significant advancements in the understanding of mixed materials in recent years.

The ability of models to correctly predict the formation conditions of mixed materials depends critically on chemical effects in the surface layers. Unfortunately, the inclusion of chemistry in kinetic models must be done in some ad hoc manner based on literature values that may not be applicable to plasma-created mixed materials. Likewise the large fluence of particles associated with plasma-facing surfaces in ITER may not be compatible with a molecular dynamics modeling approach to the mixed systems. Some technique is urgently needed to self-consistently address the issue of chemical effects with respect to plasma–surface interactions.

It is clear that the mixing of materials in plasma-facing surfaces can alter the hydrogenic retention properties of surfaces. In the W/C case, the retention level seems to lie between those expected from the pure materials. In the Be/C case, retention is increased somewhat above that expected from pure carbon. However, the largest impact on the tritium accumulation inside the ITER vessel appears to be associated with changes in the hydrogenic inventory in codeposited layers located in regions away from direct plasma contact. The composition of codeposited layers, and thereby their hydrogen retention properties, may be determined by the erosion properties of mixed materials, as has been seen in the PISCES experiments. Or the codeposited materials containing W/C or Be/C mixes may react similar to laboratory carbide formation measurements that observe the release of hydrogen when carbides form. Finally, the retention properties of the tungsten beryllides is still completely unknown and it can only be hoped that the elevated temperature required for their formation may mitigate any adverse effects.

Acknowledgements

It is my pleasure to acknowledge many useful discussions with, and suggestions from, the members of the PISCES Laboratory and our European collaborators. In particular, I would like to thank Professor Marie Doerner for her editing and, Dr Matthew Baldwin and Professor Sergei Krasheninnikov, for their input.

References

[1] ITER Technical Basis, ITER EDA Documentation Series No. 24, IAEA, Vienna, 2002.
[2] S.A. Cohen et al., J. Nucl. Mater. 76&77 (1978) 459.

[3] B.E. Mills et al., J. Nucl. Mater 162–164 (1989) 343.
[4] M. Rubel et al., J. Nucl. Mater. 313–316 (2003) 321.
[5] J. Likonen, E. Vainonen-Ahlgren, J.P. Coad, et al., J. Nucl. Mater. 337–339 (2005) 60.
[6] J.P. Coad, P.L. Andrew, A.T. Peacock, Phys. Scripta T81 (1999) 7.
[7] J.P. Coad, P. Andrew, D.E. Hole, et al., J. Nucl. Mater. 313–316 (2003) 419.
[8] G.F. Matthews, J. Nucl. Mater. 337–339 (2005) 1.
[9] B.A. Carreras, J. Nucl. Mater. 337–339 (2005) 315.
[10] S.J. Zweben, R.W. Gould, Nucl. Fusion 25 (1985) 171.
[11] A. Loarte, G. Saibene, R. Satori, et al., Phys. Plasmas 11 (5) (2004) 2668.
[12] Y. Hirooka, J. Won, R. Boivin, et al., J. Nucl. Mater. 228 (1996) 148.
[13] D.M. Goebel, Y. Hirooka, R.W. Conn, et al., J. Nucl. Mater. 145–147 (1987) 61.
[14] W. Eckstein, J. Roth, Nucl. Instrum. and Meth. B 53 (1991) 279.
[15] W. Moeller, W. Eckstein, J.P. Biersack, Comp. Phys. Commun. 51 (1988) 355.
[16] R. Kawakami, K. Ohya, Jpn. J. Appl. Phys. 40 (2001) 5399.
[17] W. Eckstein, C. Garcia-Rosales, J. Roth, W. Ottenberger, Sputtering Datt IPP Report 9/82 (1993).
[18] W. Eckstein, V.I. Shulgand, J. Roth, Nucl. Instrum. and Meth. B 153 (1999) 415.
[19] R. Kawakami, K. Ohya, Jpn. J. Appl. Phys. 42 (2003) 5259.
[20] K. Schmid, J. Roth, J. Nucl. Mater. 302 (2002) 96.
[21] Ch. Linsmeier, J. Luthin, P. Goldstrass, J. Nucl. Mater. 290–293 (2001) 25.
[22] J. Luthin, Ch. Linsmeier, J. Nucl. Mater. 290–293 (2001) 121.
[23] F.C. Sze, L. Chousal, R.P. Doerner, et al., J. Nucl. Mater. 266–269 (1999) 1212.
[24] W. Wang, V. Kh. Alimov, B.M.U. Scherzer, et al., J. Nucl. Mater. 241–243 (1997) 1087.
[25] M. Taniguchi, K. Sato, K. Ezato, et al., J. Nucl. Mater. 313–316 (2003) 360.
[26] K. Schmid, J. Roth, J. Nucl. Mater. 313–316 (2003) 302.
[27] J.W. Davis, A.A. Haasz, J. Nucl. Mater. 241–243 (1997) 37.
[28] J. Roth, R. Preuss, W. Bohmeyer, et al., Nucl. Fusion 44 (2004) L21.
[29] G. Federici, R.A. Anderl, P. Andrew, et al., J. Nucl. Mater 266–269 (1999) 14.
[30] K. Ashida, K. Fujino, T. Okabe, et al., J. Nucl. Mater. 290–293 (2001) 42.
[31] R.A. Anderl, R.J. Pawelko, S.T. Schuetz, J. Nucl. Mater. 290–293 (2001) 38.
[32] V. Kh. Alimov, Phys. Scripta T108 (2004) 46.
[33] O.V. Ogorodnikova, J. Roth, M. Mayer, J. Nucl. Mater. 313–316 (2003) 469.
[34] J.N. Brooks, J.P. Allain, T.D. Rognlien, Phys. Plasmas 13 (2006) 122502.
[35] P. Goldstrass, Ch. Linsmeier, J. Nucl. Mater. 290–293 (2001) 71.
[36] W. Eckstein, M. Hou, V.I. Shulga, Nucl. Instrum. and Meth. B 119 (1996) 477.
[37] C. Kittel, Introduction to Solid State Physics, Wiley, New York, 1976.
[38] E. Gauthier, W. Eckstein, J. Laszlo, et al., J. Nucl. Mater. 176&177 (1990) 438.
[39] P. Goldstrass, W. Eckstein, Ch. Linsmeier, J. Nucl. Mater. 266–269 (1999) 581.
[40] W. Eckstein, J. Nucl. Mater. 281 (2000) 195.
[41] R.P. Doerner, M.J. Baldwin, K. Schmid, Phys. Scripta T111 (2004) 75.
[42] K. Schmid, M. Baldwin, R. Doerner, A. Wiltner, Nucl. Fusion 44 (2004) 815.
[43] R.P. Doerner, A.A. Grossman, S.C. Luckhardt, et al., J. Nucl. Mater. 266–269 (1999) 392.
[44] K. Schmid, M. Baldwin, R. Doerner, J. Appl. Phys. 97 (2005) 064912.
[45] M.J. Baldwin, R.P. Doerner, Nucl. Fusion 46 (2006) 444.
[46] M.J. Baldwin, R.P. Doerner, K. Schmid, et al., J. Nucl. Mater. 358 (2006) 96.
[47] D. Nishijima et al., these Proceedings, doi:10.1016/j.jnucmat.2007.01.177.
[48] G. Federici, A. Zhitlukhin, N. Arkhipov, et al., J. Nucl. Mater. 337–339 (2005) 684.
[49] R. Pugno et al., these Proceedings, doi:10.1016/j.jnucmat.2007.01.243.
[50] K. Ashida, K. Watanabe, T. Okabe, J. Nucl. Mater. 241–243 (1997) 1060.
[51] J. Roth, W.R. Wampler, W. Jacob, J. Nucl. Mater. 250 (1997) 23.
[52] R.A. Anderl, G.R. Longhurst, R.J. Pawelko, et al., J. Fusion Energy 16 (1997) 95.
[53] M. Mayer, J. Nucl. Mater. 240 (1997) 164.
[54] R.A. Causey, D.S. Walsh, J. Nucl. Mater. 254 (1998) 84.
[55] M.J. Baldwin, K. Schmid, R.P. Doerner, et al., J. Nucl. Mater. 337–339 (2005) 590.
[56] A.V. Markin, V.P. Dubkov, A.E. Gorodetsky, et al., J. Nucl. Mater. 283–287 (2000) 1094.
[57] R.A. Causey, W.R. Wampler, D.S. Walsh, J. Nucl. Mater. 176&177 (1990) 992.
[58] C.R. Watts, Int. J. Powder Met. 4 (1968) 49.
[59] R.P. Doerner, M.J. Baldwin, R.A. Causey, J. Nucl. Mater. 342 (2005) 63.
[60] Ch. Linsmeier, these proceedings, doi:10.1016/j.jnucmat.2007.01.224.
[61] R.P. Doerner, S.I. Krasheninnikov, K. Schmid, J. Appl. Phys. 95 (2004) 4471.
[62] M.J. Baldwin, these proceedings, doi:10.1016/j.jnucmat.2007.01.151.
[63] M. Mayer, R. Berisch, H. Plank, et al., J. Nucl. Mater. 230 (1996) 67.
[64] H. Itoh, T. Matsudaira, S. Naka, et al., J. Mater. Sci. 22 (1987) 2811.
[65] T. Massalski (Ed.), Binary Alloy Phase Diagrams, ASM International, Metals Park, OH, 1987, p. 341.